Journal of Asian Ceramic Societies

ISSN: (Print) (Online) Journal homepage: https://www.tandfonline.com/loi/tace20

Changes in the glaze characteristics and moderate antibacterial activity of ceramic tile glazes with the addition of ZnO

Jinhyun Kim, Dooseok Jeong, Junghoon Choi & Ungsoo Kim

To cite this article: Jinhyun Kim, Dooseok Jeong, Junghoon Choi & Ungsoo Kim (2022) Changes in the glaze characteristics and moderate antibacterial activity of ceramic tile glazes with the addition of ZnO, Journal of Asian Ceramic Societies, 10:1, 241-252, DOI: 10.1080/21870764.2022.2038044

To link to this article: https://doi.org/10.1080/21870764.2022.2038044

Published online: 17 Feb 2022.

JOURNAL OF ASIAN CERAMIC SOCIETIES
2022, VOL. 10, NO. 1, 241–252
https://doi.org/10.1080/21870764.2022.2038044

THE CERAMIC SOCIETY OF JAPAN
THE KOREAN CERAMIC SOCIETY
Taylor & Francis
Taylor & Francis Group

FULL LENGTH ARTICLE

Changes in the glaze characteristics and moderate antibacterial activity of ceramic tile glazes with the addition of ZnO

Jinhyun Kim[a,b], Dooseok Jeong[a], Junghoon Choi[b] and Ungsoo Kim[b]

[a]Division of Materials Science and Engineering, Hanyang University, Seoul, Republic of Korea; [b]Korea Institute of Ceramic Engineering and Technology, Icheon, Republic of Korea

ABSTRACT

Zinc glaze forms a glossy surface or exhibits the characteristics of a crystalline glaze owing to the precipitation of fan shaped crystals, depending on the ZnO content. In this study, we fabricated tile specimens by adding 5–20 wt.% ZnO to commercial tile glaze and analyzed the changes in their surface characteristics, crystalline phase, microstructure, and ion dissolution. The effects of such changes on the antibacterial activity of the glaze were also analyzed. When the ZnO content exceeded 10 wt.%, the gloss of the glaze decreased, whereas the surface roughness and contact angle increased because the willemite crystalline phase generated in the glaze grew as it was exposed to the surface. In the glazes, reactive oxygen species (ROS) were not detected, irrespective of the ZnO content. As the ZnO content increased, the Zn ion dissolution increased, causing a change in the total dissolved ion concentration of the glaze. Furthermore, apart from the changes in the other characteristics of the analyzed glaze specimens, the antibacterial activity against *S. aureus* and *E. coli* was found to increase with the Zn ion dissolution. As reported previously, zinc ion dissolution is apparently the major cause of the antibacterial activity exhibited by these glazes.

ARTICLE HISTORY
Received 9 November 2021
Accepted 1 February 2022

KEYWORDS
Ceramic tile glaze; zinc oxide; willemite crystalline phase; ion dissolution; antibacterial activity

1. Introduction

Glazes take various forms and colors, according to the added components and the heat treatment process, and their names or applications are determined by these factors. ZnO in glazes behaves similarly to other alkaline earth oxides, but dissolves at a higher rate at low temperatures. Therefore, when a small amount of ZnO is added to a high-fire porcelain glaze, it acts as a flux that promotes the melting of other oxides, thus improving the surface roughness and gloss of the glaze [1,2]. In contrast, when a large amount of ZnO is added, it reacts with the other components of the glaze to form gahnite ($ZnAl_2O_4$) or willemite (Zn_2SiO_4) crystals that create a matte surface. Zinc-based crystalline glazes, one of the representative crystalline glazes, are produced by generating fan shaped crystals during the cooling process by saturating the glaze with ZnO.

A glaze specimen with micro/nano surface morphology due to crystallization has different physicochemical characteristics than a smooth glaze in the amorphous state. The synergistic effect of hydrophobicity and antibacterial activity has been reported by implementing micro/nano hybrid structures on the surface of glazes [3–6]. Glaze surfaces modified with β-Si_3N_4 crystals exhibit a contact angle of ~155° and reduce bacterial population > 99% for gram positive and gram negative bacteria. Antibacterial activity has also been noted for the glazes modified with copper oxide and copper.

Recently, various attempts to produce antibacterial surfaces by coating products with ZnO or using ZnO as a component have been reported [7–14]. ZnO powders, which exhibit photochemical properties, have been found to exert antibacterial activity by generating reactive oxygen species (ROS), such as hydroxyl radicals (•OH) under UV irradiation [7]. Furthermore, nano-sized ZnO powders have been reported to produce hydroxyl radicals (•OH) upon reacting with water [8]. Glasses doped with ZnO show antibacterial activity because the eluted Zn ions destroy bacterial membranes [11–13]. Willemite crystals, which are generated on the glaze surface by the reaction of ZnO with SiO_2, have been found to limit the colonization of bacteria by improving the surface hydrophobicity [14].

Studies have been conducted to apply glaze with antifouling or antibacterial activities to the surfaces of ceramic products to improve the convenience of usage [15–17]. Cu metal and copper oxide used as coloring materials in glazes have highly effective antibacterial activities, but their characteristic colors limit the product design [18,19]. Moreover, silver sol coating has limited applications due to the difficult heat treatment process and low durability of silver coatings [20]. Therefore, it is necessary to develop antibacterial materials that can be applied to glazes without any major changes in the existing manufacturing process or the implementation of various designs.

CONTACT Ungsoo Kim ukim@kicet.re.kr Korea Institute of Ceramic Engineering and Technology, Icheon 17303, Republic of Korea

In this study, we added ZnO to commercial tile glazes and analyzed the changes in their physical characteristics and antibacterial activity after heat treatment. The changes in the surface characteristics, crystalline phase, microstructure, and ion dissolution of glazes following the addition of different amounts of ZnO, and their correlations with the antibacterial activity were analyzed. Thus, the applicability of general glazes containing ZnO as an antibacterial coating was evaluated, and a universal antibacterial glaze composition and processing technology based on ZnO addition were examined.

2. Materials and methods

Different amounts (5, 10, 15, and 20 wt.%) of ZnO (D_{50} = 0.74 μm, Daejung Chemicals, Korea) were added to a glaze procured from a tile manufacturer (Daedong Tiles Co., Ltd., Cheonan, Korea), and mixed by a ball mill for 24 h. The chemical compositions of the glazes are shown in Table 1. The glaze received from the manufacturer already contained a small amount of ZnO as a flux and zircon as an opacifier. The four types of as-prepared glazes with different ZnO contents were applied to porcelain tiles of 50 mm × 50 mm dimensions and sintered in an oxidizing atmosphere. Each glaze was sprayed on to the tiles for 10s under a pressure of 45 psi using a spray gun (W-3, Daewon Co., Korea) with 1.0 mm nozzle diameter. The tiles coated with the glaze were subsequently dried at 90°C for 4 h in an oven. For comparison, specimens coated with the as-received wall tile glaze from the manufacturer were also fabricated in an oxidizing atmosphere. For heat treatment, the specimens were heated at the rate of 3°C/min, maintained at 1100°C for 1 h, and then cooled naturally. Figure 1 summarizes the specimens used in this study.

Table 1. Chemical compositions of the glazes under investigation.

Wt.%	SiO_2	ZrO_2	Al_2O_3	B_2O_3	Na_2O	K_2O	CaO	MgO	ZnO
Zn0	54.11	6.94	7.46	7.61	2.06	4.19	9.78	2.47	5.39
Zn5	51.38	6.59	7.08	7.22	1.95	3.98	9.29	2.34	10.15
Zn10	48.66	6.24	6.71	6.84	1.85	3.77	8.80	2.22	14.92
Zn15	45.94	5.89	6.33	6.46	1.75	3.56	8.31	2.10	19.67
Zn20	43.22	5.55	5.96	6.08	1.64	3.35	7.81	1.97	24.43

The specular reflection at 60° was measured to evaluate the gloss of the glaze (Glossmeter, micro-TRI-gloss, BYK Gardner, Germany). The line roughness of glaze (R_a) was measured five times using a surface roughness tester (Surftest SJ-410, Mitutoyo, Japan) and the average value is reported. The water contact angle of the glaze surface was measured using a droplet of distilled water (SmartDrop, Femtobiomed, Korea). The surface free energy of the glaze was calculated using Neumann's equation based on the water advancing contact angle and the surface tension of distilled water [21]. After soaking the glaze specimens in a 10 mM NaCl solution, into which monitoring particles were injected, the zeta potential of the glaze surface was measured using a flat-surface zeta cell unit (ELSZ, Otsuka Electronics, Japan).

X-ray diffraction (XRD) of the glaze surface was performed using a Dmax-2500 diffractometer (Rigaku, Japan) to analyze the crystalline phase. The XRD patterns were recorded at the scan speed of 10°/min in the diffraction angle range of $10° \leq 2\theta \leq 80°$. After coating the glaze surface with platinum, the microstructure was observed by field emission scanning electron microscopy (FE-SEM; JSM-7610 F Plus, JEOL, Japan) and the composition was analyzed by energy-dispersive X-ray spectroscopy (EDS, Oxford Instruments, UK). Polished cross-sections of glazed samples were also analyzed by SEM-EDS.

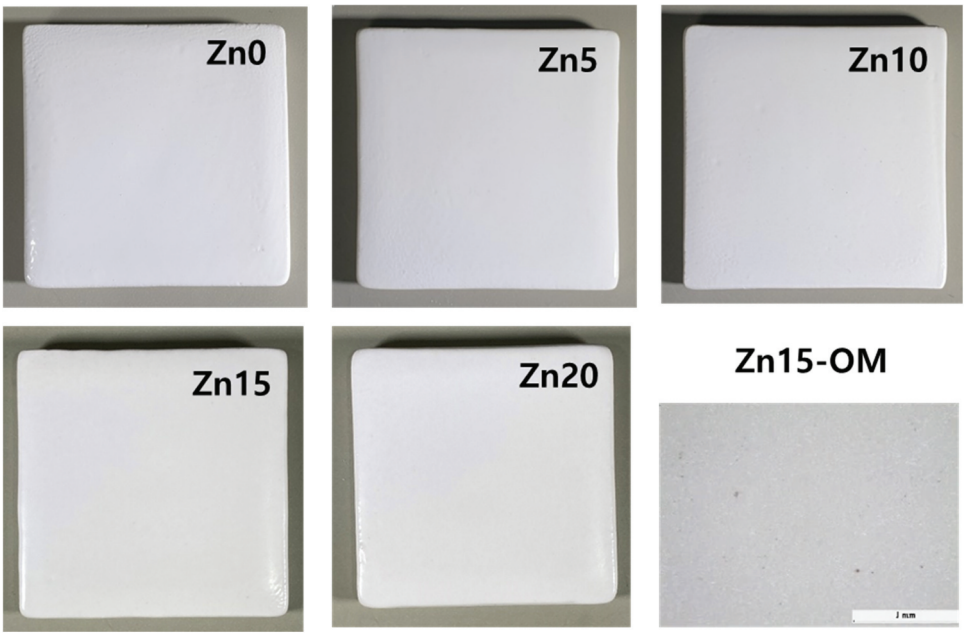

Figure 1. Porcelain tiles coated with commercial wall tile glazes with extra ZnO added.

Cup-like specimens were fabricated to analyze the dissolution characteristics of the glaze. In a typical experiment, 45 g of distilled water was stored in three replicate specimens for each condition for 24 h, and then the compositions of various specimens were analyzed by inductively coupled plasma-optical emission spectrometry (Optima 5300DV, Perkin Elmer, USA). The ROS generated on the glaze surface were analyzed using a terephthalic acid solution (TA) [22,23]. TA is known to generate fluorescent 2-hydroxyterephthalate by reacting with •OH. A solution obtained by dissolving 2 mM TA and 5 mM NaOH was placed in the cup-shaped specimens, and the setup was stored in a black box for 24 h. Then, the emission peak of 2-hydroxyterephthalate at 425 nm was analyzed under 312 nm excitation using a fluorescence analyzer (FP-8500, Jasco, Japan).

The antibacterial activity of the glaze was evaluated in accordance with the JIS Z 2081/ISO 22196 standard. *Staphylococcus aureus* ATCC 6538P (*S. aureus*, Gram positive) and *Escherichia coli* ATCC 8739 (*E. coli*, gram negative) were inoculated on separate glaze surfaces, and then microbial growth inhibition and bactericidal properties of the surfaces were evaluated. Test microorganisms were prepared by growing them in a liquid culture medium. The control and test surfaces were inoculated three times with the microorganisms, and then covered with a thin sterile film. The antibacterial activity was calculated using Eq. (1).

$$R = [log(B/A) - log(C/A)] \quad (1)$$

where R represents the antibacterial activity, A is the average number of viable bacterial cells immediately after inoculation on the untreated test specimen, B is the average number of viable bacterial cells on the untreated test specimen after 24 h, C is the average number of viable bacterial cells on the antimicrobial test specimen after 24 h.

When the R value was > 2, the antibacterial activity was deemed to be 99.9%. Under each condition, six tile specimens were analyzed and the average value for each is reported.

3. Results

The glaze specimens are displayed in Figure 1. The specimens Zn0, Zn5, and Zn10 have the properties of an opaque gloss glaze. In the cases of Zn15 and Zn20, the formation of crystalline phase on the glaze surface could be observed with the naked eye. Zn15-OM shows the crystalline phase observed under a stereomicroscope.

Table 2 lists the surface roughness, gloss, contact angle, surface free energy, and zeta potential values of the glazes. All the glazes exhibited low surface roughness (below 1 μm); however, the surface roughness increased with increasing ZnO content, and a significantly higher roughness was observed at a ZnO content of 15 wt.% or higher. The specimens showed the characteristic gloss values of glossy glaze (74–89 GU) up to a ZnO content of 10 wt.%; the gloss decreased below 20 GU at ZnO content of 15 wt.% or higher. The surface contact angles of all the glazes were smaller than 50°, indicating their hydrophilic nature. The surface free energy was found to generally increase with increasing ZnO content. The zeta potentials of all the glazes were higher than −10 mV. As the ZnO content increased, the zeta potential decreased at first and then reached a plateau.

XRD patterns of the ZnO-added glazes are shown in Figure 2. The Zn0 specimen provided peaks of zircon ($ZrSiO_4$) and diopside ($MgCaSi_2O_6$) crystalline phases, in addition to an amorphous halo. Zn5 and Zn10 provided the peaks of the zircon phase, whereas Zn15 and Zn20 provided the peaks of the willemite (Zn_2SiO_4) crystalline phase, in addition to those of the zircon phase. Thus, the crystalline phases in the samples appears to be affected by the composition (i.e. ZnO content) of the glaze. Peculiarly, the peaks of the crystalline ZnO phase did not appear under any condition. Apparently, the added ZnO dissolved to form Zn ions, or formed willemite phase by reacting with the SiO_2 melt. It has been reported that ZnO is converted to willemite crystals over a dwell time of 5 min at 1100°C [14]. The zircon used for the opacification of glaze prevailed without dissolving in all of the specimens, owing to its high thermal stability.

The SEM images of the glaze surfaces (Figure 3) revealed that Zn0 comprises irregular cuboid crystals exposed on the glass matrix surface. EDS mapping of this sample revealed that diopside crystals were formed. For Zn5 and Zn10, needle-shaped zircon crystals were observed inside the glass matrix, while for Zn15 and Zn20, longer needle-shaped crystals grew along the surface. EDS mapping images of the surfaces of Zn15 and Zn20 indicated the formation of the willemite phase. The results of SEM-EDS analyses were consistent with the XRD results. The glass matrix of

Table 2. Line roughness, gloss, contact angle, and zeta-potential values of the ceramic tile glazes with added ZnO.

Properties	Zn0	Zn5	Zn10	Zn15	Zn20
Roughness (μm)	0.35 ± 0.10	0.12 ± 0.07	0.23 ± 0.08	0.71 ± 0.06	0.69 ± 0.07
Gloss (GU)	84.4 ± 4.0	89.4 ± 1.3	74.2 ± 3.6	14.6 ± 3.1	16.1 ± 1.7
Contact Angle (°)	36.4 ± 8.4	27.0 ± 7.5	31.4 ± 3.5	47.1 ± 2.5	46.6 ± 2.2
Surface Free Energy (mJ/m^2)	4.5 ± 0.6	3.0 ± 0.2	4.5 ± 0.3	5.3 ± 0.2	5.8 ± 0.5
Zeta-Potential (mV)	−14.72 ± 0.6	−10.72 ± 0.7	−10.09 ± 0.8	−10.66 ± 0.7	−11.98 ± 0.4

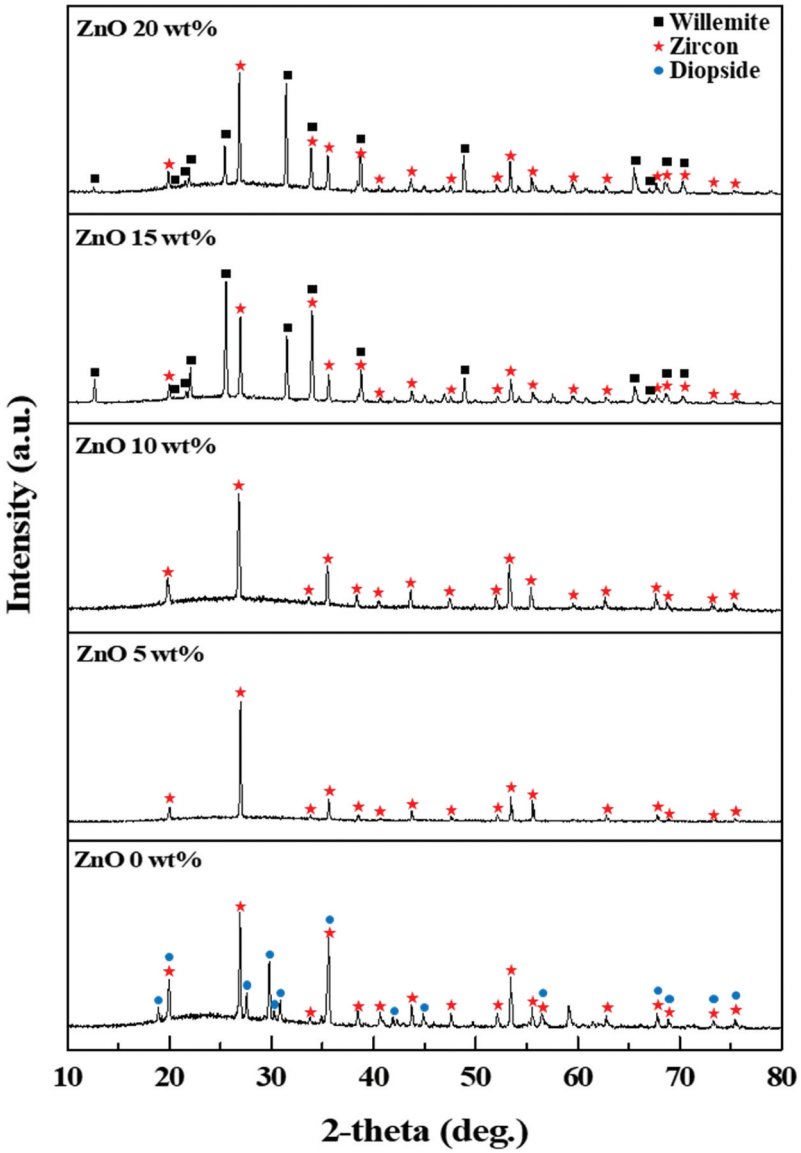

Figure 2. XRD patterns of ceramic tile glazes with added ZnO.

every glaze was found to be an aluminosilicate glass containing alkali metal ions, alkaline earth metal ions, and Zn^{2+} ions.

Figure 4 shows the micrographs of the polished-cross sections of glazes. The thickness of the glaze ranged from 98 μm (Zn10, Zn20) to 228 μm (Zn0). In the cases of Zn0, Zn5, and Zn10 specimens, the crystals were embedded within the glaze layer, while in the cases of Zn15 and Zn20, crystals were found both within the matrix and on the surface of the glaze layer. EDS mapping of the glaze indicated that Zn ions were uniformly distributed in the glaze layer.

The ion dissolution behaviors of the glaze specimens are presented in Table 3. Distilled water mixed with diluted nutrients was used for cultivating bacteria in the antibacterial tests, and different nutritional compositions were used for the two types of bacteria tested. Although the compositions of the two bacterial media used for ion dissolution measurements were different, the dissolution environment of the glaze can be considered equivalent because the bacterial medium was designed to provide only bare minimum nutrients to the bacteria during antibacterial test and the nutrient concentration was maintained at a very low level (1.6×10^{-6} g/mL).

The total dissolved ion concentration decreased as the ZnO content increased to 10 wt.%, and increased again when the ZnO content increased further. Zn0 had the highest dissolved Ca ion content (0.102 mg/L), whereas Zn15 had the highest dissolved Zn ion content (0.076 mg/L) among the samples. In general, the dissolution quantity was the highest for Na^{+}, followed by those of K^{+} and Zn^{2+}.

The results of the ROS analysis are summarized in Figure 5. Regardless of the ZnO content, •OH was not found in any specimen. Although not shown here, the characteristic fluorescence of 2-hydroxyterephthalate at 425 nm did not appear in the preliminary experiment conducted with 5, 10, and 50 mM of TA for

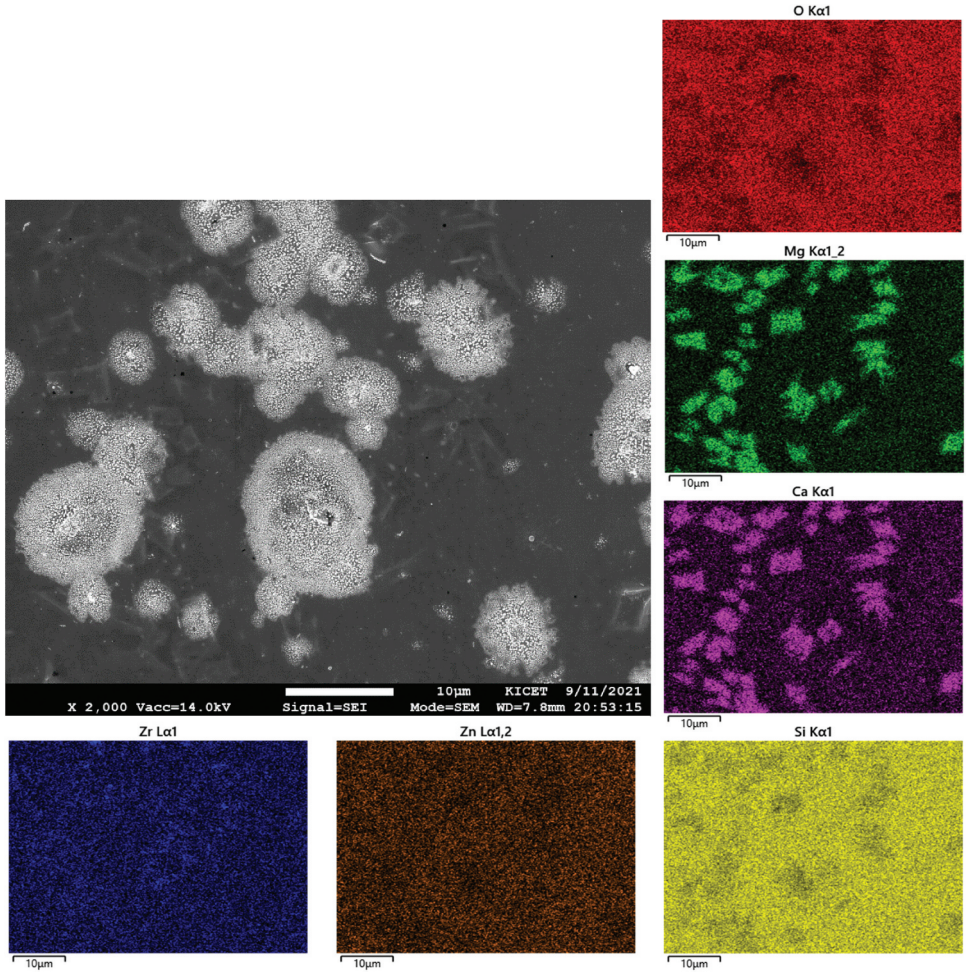

Figure 3. Micrographs of glaze surfaces and the corresponding EDS mapping images: (a) Zn0, (b) Zn5, (c) Zn10, (d) Zn15, and (e) Zn20.

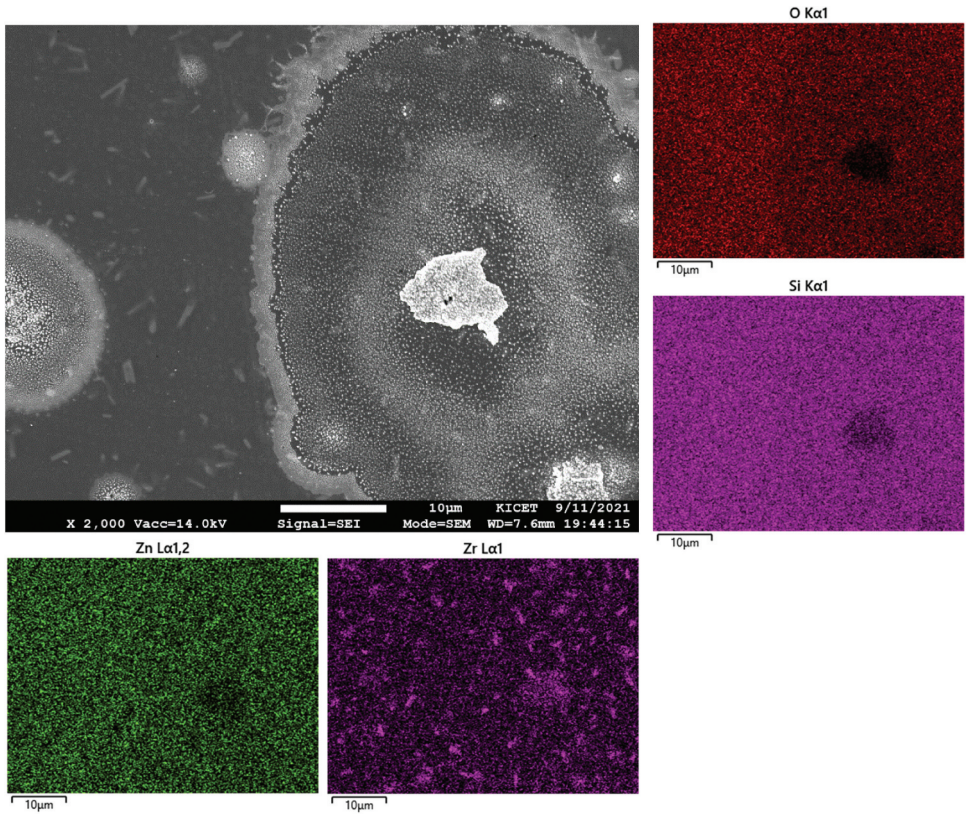

Figure 3. (Continued)

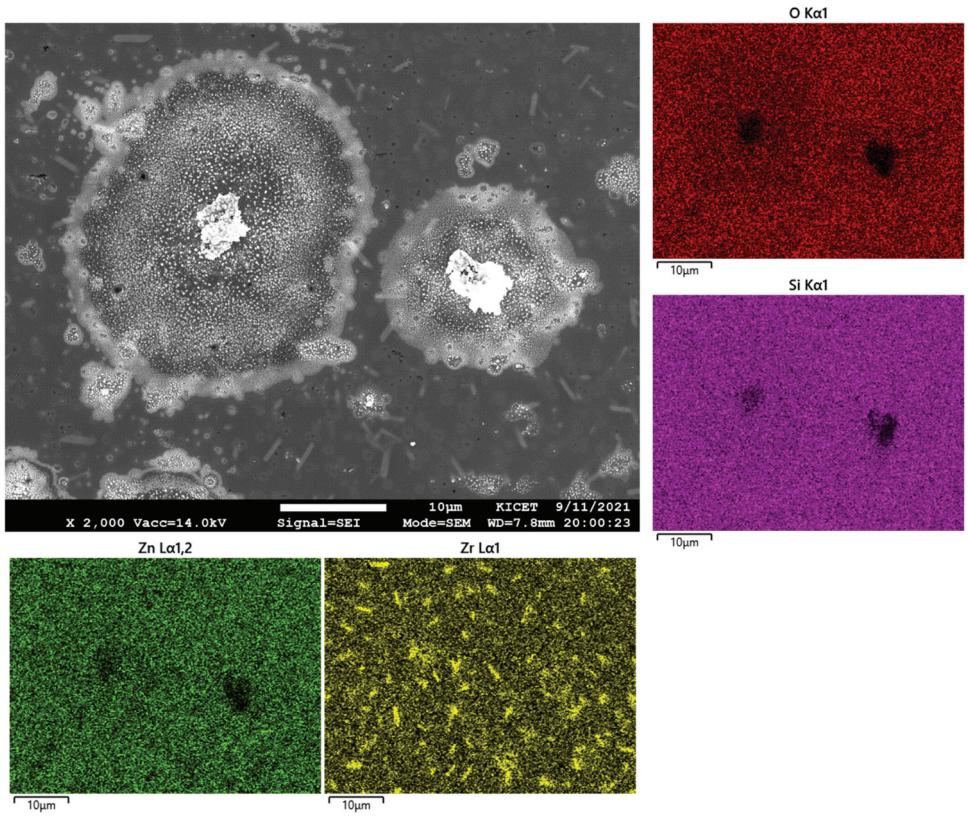

Figure 3. (Continued)

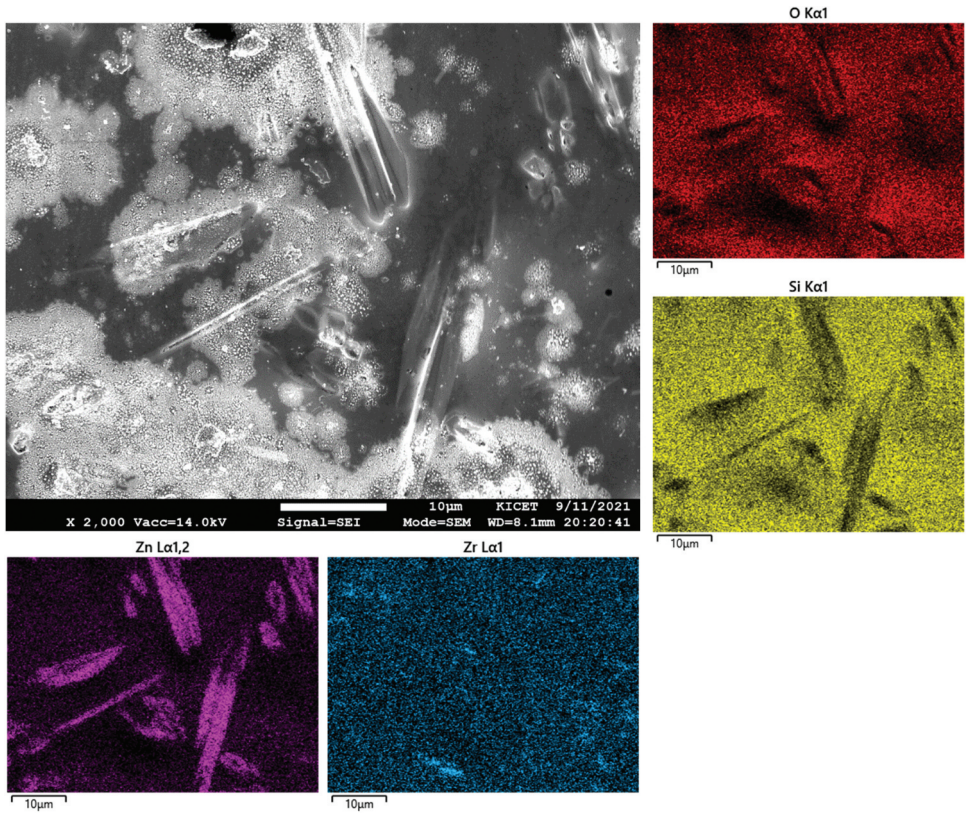

Figure 3. (Continued)

concentration optimization. It was therefore inferred that ROS was not generated on the glaze surface, regardless of the ZnO content.

Table 4 summarizes the antibacterial properties of the different glazes. Zn0 showed an antibacterial activity of 83.4% against *S. aureus*, but Zn5 showed

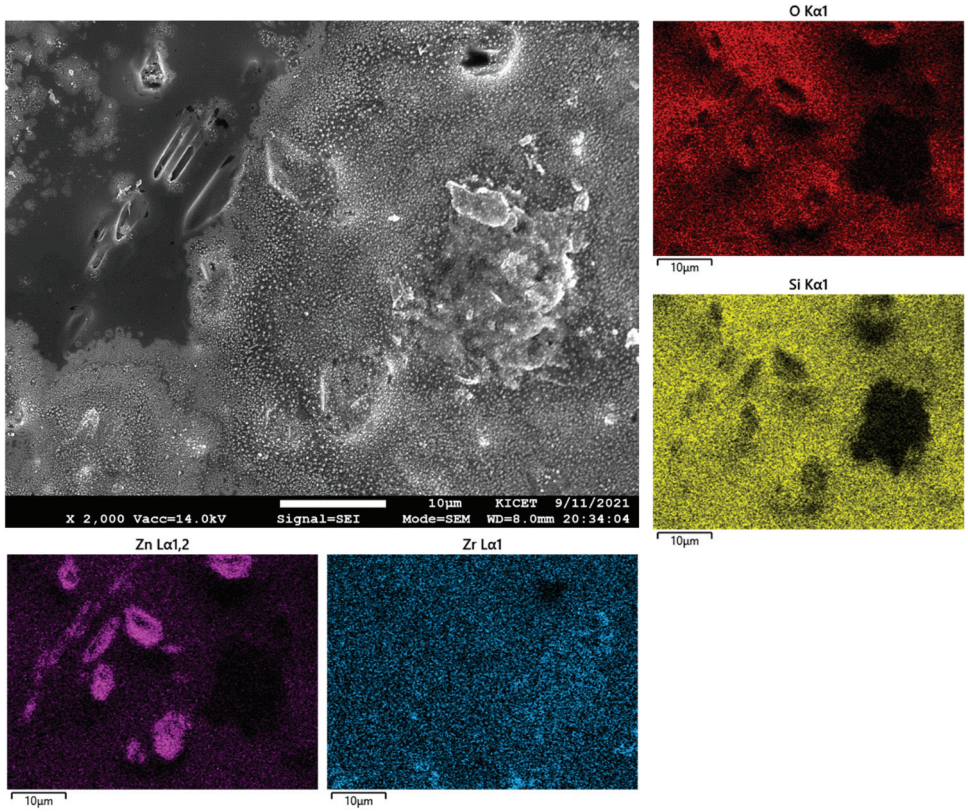

Figure 3. (Continued)

a reduced antibacterial activity of 27.5%. As the ZnO content increased, the antibacterial activity of Zn20 against *S. aureus* increased to 89.4%. The antibacterial activity of the glaze against *E. coli* increased with increasing ZnO content. The antibacterial activity of Zn10 was higher than 73%, while that of Zn20 was close to 90%.

4. Discussion

XRD and SEM-EDS studies suggested that irregular cuboid crystals of diopside were formed on the glaze surface at a low ZnO concentration (Zn0), while needle-shaped willemite crystals were formed at a relatively high ZnO concentration (Zn15, Zn20). At intermediate ZnO concentrations (Zn5 and Zn10), crystals were observed on the glaze surface, only zircon crystals were present within the glaze layer.

Figure 6 correlates the ZnO content, surface roughness, and contact angle of the glazes. The surface roughness and contact angle of the glaze increased with the addition of ZnO. The willemite phase appearing on the surface of the glaze at ZnO contents exceeding 15 wt.% formed nano- or micro-sized crystals, leading to increased surface roughness. The water contact angle of the glaze surface with nano- or micro-sized structures increased possibly because of the so-called lotus effect.

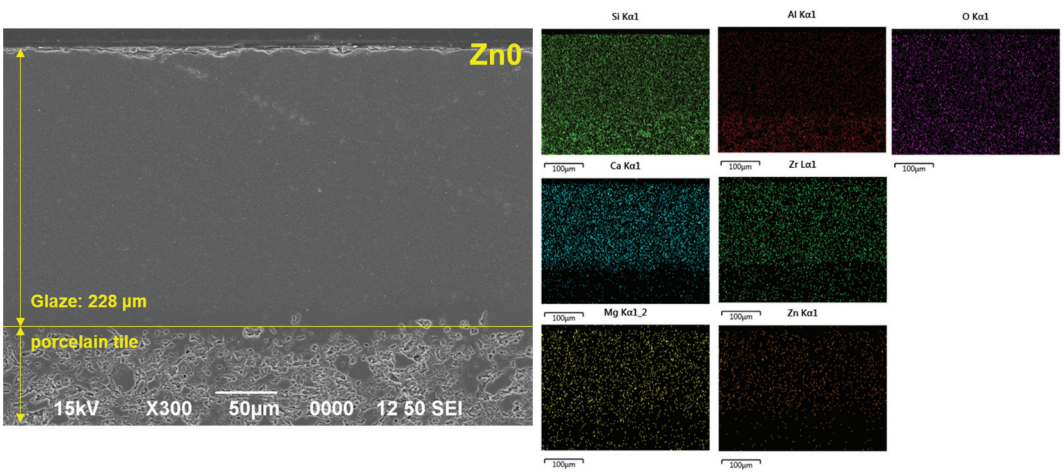

Figure 4. Micrographs of the polished cross-sections of glazes: (a) Zn0, (b) Zn5, (c) Zn10, (d) Zn15, and (e) Zn20.

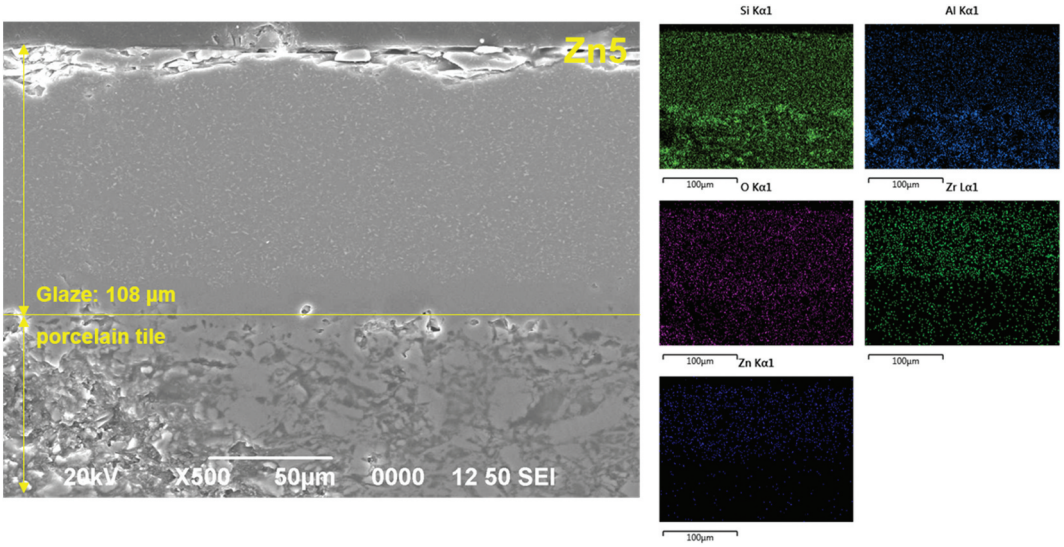

Figure 4. (Continued)

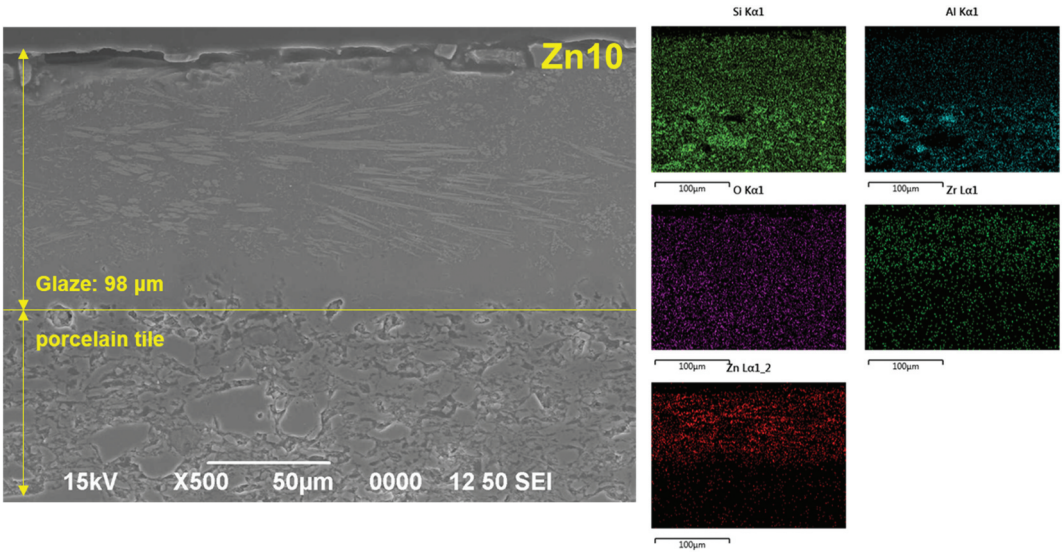

Figure 4. (Continued)

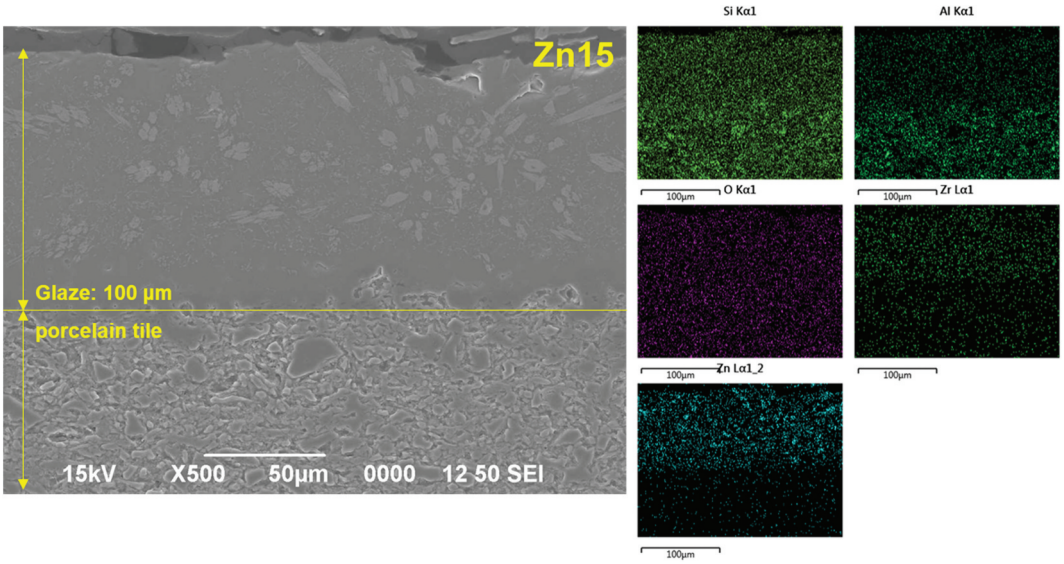

Figure 4. (Continued)

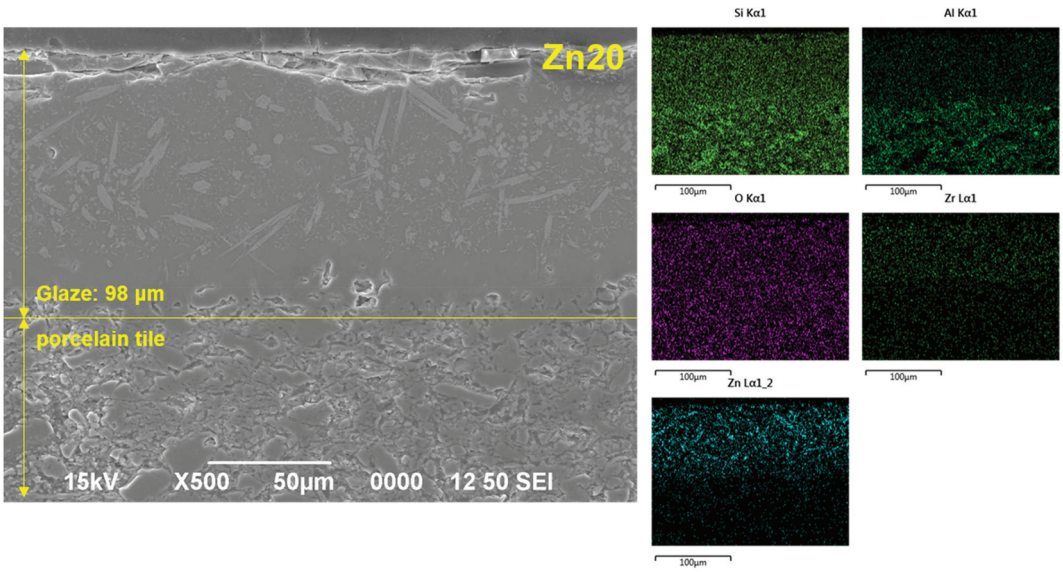

Figure 4. (Continued)

Table 3. Dissolved ion concentrations (mg/L) of ceramic tile glazes with added ZnO.

Sample	Si	B	Na	K	Ca	Mg	Zn	Total
Zn0	0.029	0.010	0.425	0.076	0.102	0.004	0.002	0.646
Zn5	0.031	0.009	0.470	0.071	0.013	0.002	0.002	0.596
Zn10	0.030	0.008	0.455	0.069	0.009	0.003	0.006	0.578
Zn15	0.047	0.008	0.445	0.080	0.057	0.008	0.076	0.721
Zn20	0.047	0.008	0.445	0.074	0.012	0.008	0.075	0.666

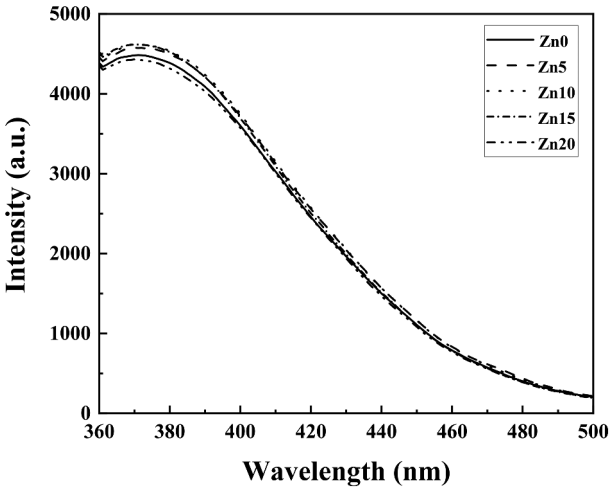

Figure 5. Fluorescence spectra of terephthalic acid solutions stored for 24 h in ceramic cups made of tile glazes under dark conditions.

Table 4. Antibacterial properties of ceramic tiles with added ZnO.

Antibacterial activity		Zn0	Zn5	Zn10	Zn15	Zn20
Staphylococcus aureus	(%)	83.4	27.5	72.2	79.4	89.4
	R (log)	0.8	0.1	0.5	0.7	1.0
Escherichia Coli	(%)	0	21.1	73.4	80.7	89.1
	R (log)	0	0.1	0.6	0.7	1.0

Figure 7 shows the correlation between the surface roughness, gloss, and contact angle of the glaze. As the surface roughness increased from 0.354 to 0.687 μm,

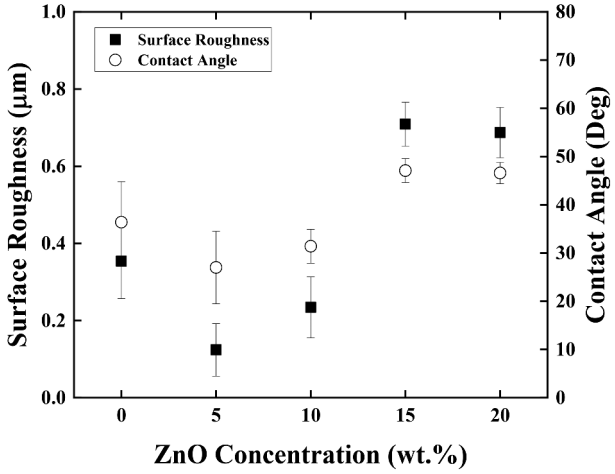

Figure 6. Surface roughness and contact angle values of tile glazes at different ZnO contents.

the gloss decreased from 84.4 to 16.1 GU and the contact angle increased from 36.4 to 46.6 °. The diopside and willemite crystals precipitated on the surface scatter light, thus lowering the gloss value [24]. Furthermore, nano- or micro-sized features on the surface increase the hydrophobic property of the surface by inducing the lotus effect. Consequently, the increase in surface roughness due to the crystallization of certain phases led to increased contact angle [25,26].

Figure 8 shows that the antibacterial activity increases with increasing contact angle of the glaze. However, considering the results of previous studies on the origin of antibacterial activity, a surface with a high contact angle apparently provides an environment that is disadvantageous for the survival of bacteria rather than being a direct cause of killing bacteria. A study on the adhesion of bacteria to glass surfaces indicated that bacterial adhesion hardly depended on the surface charge of glass, but significantly on the

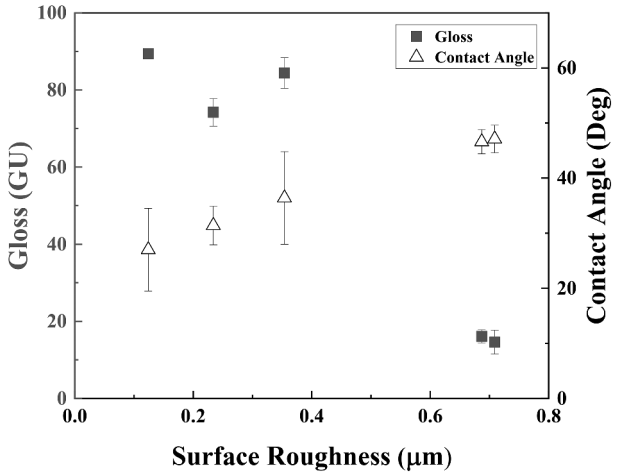

Figure 7. Relationship between the surface roughness, gloss, and contact angle of tile glazes.

contact angle (i.e. hydrophobicity) [27]. In other words, a relatively rough surface with increased contact angle facilitates the adhesion of bacteria to the glaze surface, which provides an environment that suppresses the growth and proliferation of bacteria.

Figure 9 shows the ion dissolution behavior of the glaze at different ZnO contents. When the ZnO content increased, both the dissolved Zn ion concentration and the total dissolved ion concentration increased. However, when the dissolution of ions other than Zn ions was examined, the increase in Zn ion dissolution appeared to cause the increase in the total concentration of dissolved ions. The dissolution property of glaze is speculated to be strongly related to the composition and structural change of the glassy phase that appears when the ZnO content increases, rather than with the crystalline phase generated on the surface.

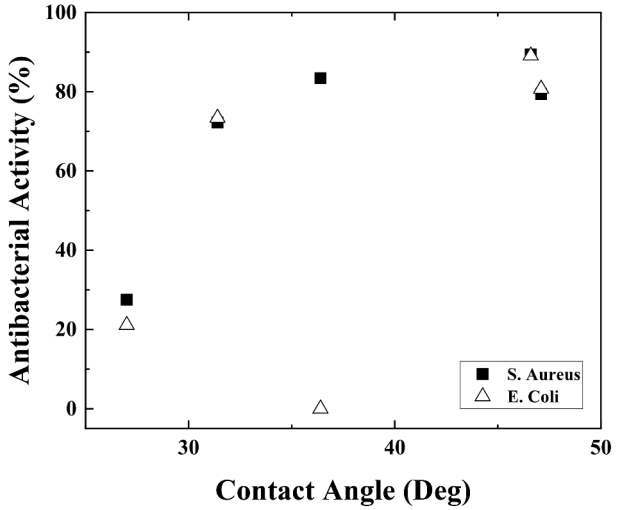

Figure 8. Antibacterial activities of tile glazes at different contact angles.

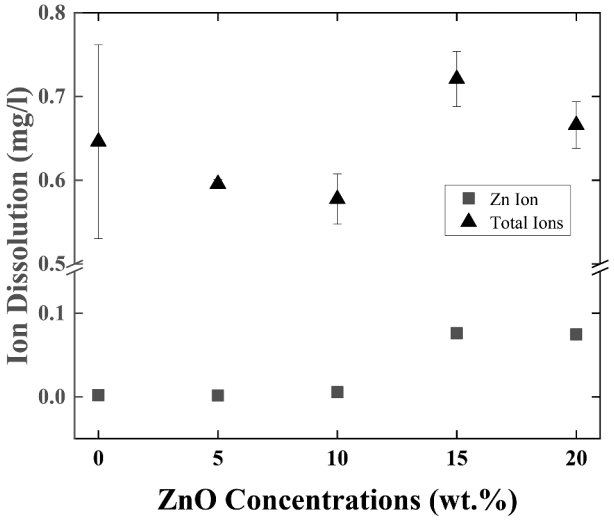

Figure 9. Ion dissolution behavior of tile glazes at different ZnO contents.

In a previous study that comparing the dissolution rates of glass and crystalline phases of the same composition, a significant effect of the atomic ordering and structure on solid reactivity was observed [28,29]. In other words, the glass phase, which does not have a long-range structure, showed a higher dissolution rate than the ordered crystalline phase. As the ZnO content increased, the content of non-bridging oxygen in the glaze increased, which in turn enhanced the depolymerization of the glassy network [30,31]. Therefore, the glass phase formed with the dissolution of ZnO in the glaze matrix appears to contribute to the increase in the dissolved Zn ion concentration more than the crystalline phases formed on the surface upon ZnO addition.

Figure 10 shows that, as the dissolved Zn ion concentration increased, the antibacterial activity against both *S. aureus* and *E. coli* increased with a similar trend. The dissolved Zn ions show antibacterial activity by destroying the bacterial membranes [7–9]. However, the dissolved concentration of the Zn ion, which shows antibacterial activity, in the specimens studied herein is considerably lower than the concentration reported in earlier studies. The Zn ion concentration required for 80% or higher antibacterial activity against *S. aureus* and *E. coli* is 0.65–6.54 mg/L [32]. Therefore, certain factors other than Zn ion dissolution are responsible for the antibacterial properties of the ZnO-added glaze, which shows significant antibacterial activity even at low dissolved Zn ion concentration. Vincent et. al. claimed that cell surfaces are damaged by even trace amounts of ions that dissolve when the bacteria are in contact with the surface [33]. Therefore, the increased contact angle, which was previously identified as an indirect factor is considered to facilitate the adhesion of bacteria to the glaze surface, and the Zn ions dissolved from the surface have a antibacterial effect by directly destroying the bacterial membranes.

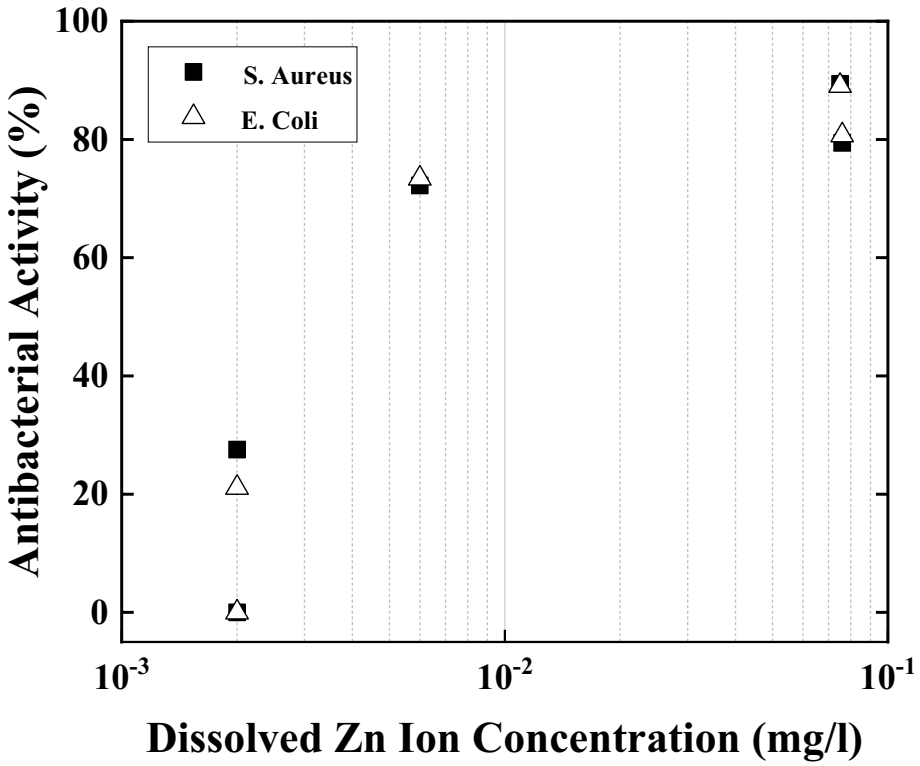

Figure 10. Antibacterial activities of tile glazes at different dissolved Zn ion concentrations.

5. Conclusions

The effect of the change in the characteristics of a commercial wall tile glaze with ZnO addition (5–20 wt.%) on the antibacterial activity of the glaze surface was analyzed. As the ZnO content increased, the gloss of the ceramic tile decreased, whereas the surface roughness and contact angle increased. XRD and SEM-EDS analyses indicated that, when the ZnO content exceeded 15 wt.%, willemite crystalline phase was formed inside the glaze and was exposed on the surface, where it grew. The crystalline phases exposed on the surface appeared to increase the surface roughness and contact angle, while reducing the gloss. Furthermore, as the ZnO content increased, the dissolved Zn ion concentration increased, in turn increasing the total dissolved ion concentration of the glaze. The dissolved concentration of other ions, excluding Zn ions, was maintained at similar levels, regardless of the ZnO content.

To determine the cause of the antibacterial activity exhibited by the glaze, the relationship between the glaze properties and antibacterial activity was analyzed. As the contact angle and the dissolved Zn ion concentration of the glaze increased, the antibacterial activities against both *S. aureus* and *E. coli* increased to 89% with a similar trend. Considering the results of previous studies on the antibacterial mechanism of Zn-containing glazes, the dissolved Zn ions are apparently the major cause of the antibacterial activity.

Acknowledgments

This work was supported by the National Research Foundation of Korea (NRF) grant funded by the Korea government (MSIT; Grant No. 2018M3C1B505215).

Disclosure statement

No potential conflict of interest was reported by the author(s).

Funding

This work was supported by the National Research Foundation of Korea [2018M3C1B505215].

References

[1] Parmelee CW. Ceramic glazes. Boston (MA): Cahners Books; 1973.
[2] Eppler RA, Eppler DR. Glazes and glass coatings. Westerville (OH): American Ceramic Society; 2000.
[3] Acikbas G, Acikbas NC. The effect of sintering regime on superhydrophobicity of silicon nitride modified ceramic surfaces. J Asian Ceram Soc. 2021;9(2):734–744.
[4] Acikbas G, Acikbas NC. Copper oxide-and copper-modified antibacterial ceramic surfaces. J Am Ceram So. 2022;105(2):873–887.
[5] Acikbas G, Acikbas NC. Nanoarchitectonics for polymer-ceramic hybrid coated ceramic tiles for antibacterial activity and wettability. Appl Phys A. 2021;127(10):794.

[6] Özcan S, Acikbas NC, Acikbs G. Formation of antibacterial effect on ceramic tile surfaces. Anadolu Univ J Sci Technol A. 2017;18(1):122–130.
[7] Park KH, Han GD, Neoh KC, et al. Antibacterial activity of the thin ZnO film formed by atomic layer deposition under UV-A light. Chem Eng J. 2017;328(15):988–996.
[8] Applerot G, Lipovsky A, Dror R, et al. Enhanced antibacterial activity of nanocrystalline ZnO due to increased ROS-mediated cell injury. Adv Funct Mater. 2009;19(6):842–852.
[9] Applerot G, Perkas N, Amirian G, et al. Coating of glass with ZnO via ultrasonic irradiation and a study of its antibacterial properties. Appl Surf Sci. 2009;256(3):S3–S8.
[10] Yi G, Yuan Y, Li X, et al. ZnO nanopillar coated surfaces with substrate-dependent superbactericidal property. Small. 2018;14(14):1703159 1–8.
[11] Esteban-Tejeda L, Prado C, Cabal B, et al. Antibacterial and antifungal activity of ZnO containing glasses. PloS ONE. 2015;10(8):e0136490.
[12] Wajda A, Goldmann WH, Detsch R, et al. Influence of zinc ions on structure, bioactivity, biocompatibility and antibacterial potential of melt-derived and gel-derived glasses from CaO-SiO_2 system. J Non-Cryst Solids. 2019;511(1):86–99.
[13] Sánchez-Salcedo S, Shruti S, Salinas AJ, et al. In vitro antibacterial capacity and cytocompatibility of SiO_2–CaO–P_2O_5 meso-macroporous glass scaffolds enriched with ZnO. J Mater Chem B. 2014;2(30):4836–4847.
[14] Özcan S, Açikbaş G, Açikbaş AC. Induced superhydrophobic and antimicrobial character of zinc metal modified ceramic wall tile surfaces. Appl Surf Sci. 2018;438 (30):136–146.
[15] Knies F, Schrantz K, Aneziris C, et al. Superhydrophilic ceramic glazes for sanitaryware. J Ceram Sci Technol. 2016;07(1):53–64.
[16] Seabra MP, Grave L, Oliveira C, et al. Porcelain stoneware tiles with antimicrobial action. Ceram Int. 2014;40 (4):6063–6070.
[17] De Niederhäusern S, Bondi M, Bondioli F. Self-cleaning and antibacteric ceramic tile surface. Int J Appl Ceram Technol. 2013;10(6):949–956.
[18] Hans M, Erbe A, Mathews S, et al. Role of copper oxides in contact killing of bacteria. Langmuir. 2016;29 (52):16160–16166.
[19] Choi J, Kim J, Han K, et al. Antibacterial behavior of copper glazes: effect of copper(II) oxide concentrations and sintering atmospheres. J Korean Ceram Soc. 2021;58(3):287–296.
[20] Baheiraei N, Moztarzadeh F, Hedayati M. Preparation and antibacterial activity of Ag/SiO_2 thin film on glazed ceramic tiles by sol-gel method. Ceram Int. 2012;38(4):2921–2925.
[21] Li D, Neumann AW. Contact angles on hydrophobic solid surfaces and their interpretation. J Colloid Interface Sci. 1992;148(1):190–200.
[22] Lakshmi Prasanna V, Vijayaraghavan R. Insight into the mechanism of antibacterial activity of ZnO: surface defects mediated reactive oxygen species even in the dark. Langmuir. 2015;31(33):9155–9162.
[23] Xu X, Chen D, Yi Z, et al. Antimicrobial mechanism based on H_2O_2 generation at oxygen vacancies in ZnO crystals. Langmuir. 2013;29(18):5573–5580.
[24] Gim J, Rhee B. Generation mechanism of gloss defect for high-glossy injection-molded surface. Korea Aust Rheol J. 2020;32(3):183–194.
[25] Cheng YT, Rodak DE, Wong CA, et al. Effects of micro- and nano-structures on the self-cleaning behaviour of lotus leaves. Nanotechnology. 2006;17 (5):1359–1362.
[26] Yang C, Tartaglino PBN, Persson BNJ. Influence of surface roughness on superhydrophobicity. Phys Rev Lett. 2006;97(11):116103-1-4.
[27] Li B, Logan BE. Bacterial adhesion to glass and metal-oxide surfaces. Colloids Surf B. 2004;36(2):81–90.
[28] Perez A, Daval D, Fournier M, et al. Comparing the reactivity of glasses with their crystalline equivalents: the case study of plagioclase feldspar. Geochim Cosmochim Acta. 2019;254(1):122–141.
[29] Chang HY, Lin CC, Shen P, et al. Dissolution of willemite polycrystals: effects of pH, temperature and TiO_2 solid solution. J Mater Sci. 1993;28(7):1781–1787.
[30] Leśniak M, Partyka J, Gajek M, et al. FTIR and MAS NMR study of the zinc aluminosilicate ceramic glazes. J Mol Struct. 2018;1171(5):17–24.
[31] Leśniak M, Partyka J, Sitarz M, et al. Impact of ZnO on the structure of aluminosilicate glazes. J Mol Struct. 2016;1126(15):251–258.
[32] Ning C, Wang X, Li L, et al. Concentration ranges of antibacterial cations for showing the highest antibacterial efficacy but the least cytotoxicity against mammalian cells: implications for a new antibacterial mechanism. Chem Res Toxicol. 2015;28 (9):1815–1822.
[33] Vincent M, Hartemann P, Engels-Deutsch M. Antimicrobial applications of copper. Int J Hyg Environ Health. 2016;219(7):585–591.